
Detecting windmill parks in the ocean on Sentinel satellite imagery

Aelbrecht Rudolf Leclercq Frederic

Abstract

In this paper we will try to identify windmill parks in the ocean based on satellite imagery. A convolutional neural network (CNN) was trained to detect individual windmills and boats. Land coverage maps and noise reduction techniques were applied in the preprocessing phase to improve training. Density-based clustering algorithms (DBSCAN and OPTICS) were compared in order to optimize the intermediate results. The final result is a generated Esri-shapefile that encircles all identified parks with a polygon.

1. Introduction

The Sentinel-1 mission is the European Radar Observatory for the Copernicus joint initiative of the European Commission (EC) and the European Space Agency (ESA). Copernicus is a European initiative for the implementation of information services dealing with environment and security. It is based on observation data received from Earth Observation satellites and ground-based information.

The Sentinel-1 mission includes C-band imaging operating in four exclusive imaging modes with different resolutions (down to 5 m) and coverage (up to 400 km). It provides dual polarization capability, very short revisit times and rapid product delivery. For each observation, precise measurements of the spacecraft's position and attitude are available.

Synthetic Aperture Radar (SAR) has the advantage of operating at wavelengths not impeded by cloud cover or a lack of illumination and can acquire data over a site during day or night time under all weather conditions. Sentinel-1, with its C-SAR instrument, offers reliable, repeatable wide area monitoring.

The Sentinel-1 products are freely downloadable in GeoTIFF format. GeoTIFF is a public domain metadata standard which allows georeferencing information to be embedded within a TIFF file. The potential additional information includes map projection, coordinate systems, ellipsoids, data, and everything else necessary to establish the exact spatial reference for the file.

We aim to detect windmill parks in the ocean based on this

satellite imagery.

2. Related work

The most relevant project we found to what we set out to do is a project developed in Duke University that is planning to map the energy infrastructure of the world using satellite imagery ([duk, 2020a](#)). They began with mapping all windmills in the USA and explained their approach ([duk, 2020b](#)) using a combination of machine learning and simulated imagery. They applied their models to colored satellite imagery and got satisfactory results. The project has at the point of writing this paper not expanded to any other areas or ocean based windmills. The project was also much larger in scale than what we set out to do, so we the idea of generating artificial imagery to train our model was not an option.

Another related project is written on Medium ([Moraite, 2019](#)) which explained how it is relatively easy to identify ships using a CNN. This article has no sources for its data set due to link-rot; we assume it is related to another project using a different approach ([Sagar, 2019](#)). In both cases we can see that they used high resolution color satellite imagery. Both examples did not test on larger datasets, so we can assume that the model would probably not perform as well in a real world scenario. It gave us however a good example in how detecting ocean object can be done with even a simple neural network.

3. Method

Compared to the existing work, we noticed that while looking at repositories of satellite imagery that cloudless imagery is quite rare and not feasible to parse on a global scale, since a lot of areas are missing. This is one of the reasons that we chose to use single channel image data from Sentinel, which is not affected by weather. Another disadvantage we had with our data set is that the resolution is quite low, and glare makes it at times hard to distinguish objects.

To lack of resolution and clarity made it hard to discern the

055
056
057
058
059
060
061
062
063
064
065
066
067
068
069
070
071
072
073
074
075
076
077
078
079
080
081
082
083
084
085
086
087
088
089
090
091
092
093
094
095
096
097
098
099
100
101
102
103
104
105
106
107
108
109

shape of a windmill and thus to train a neural net to identify the distinct shape of a windmill. We therefore decided to focus on detecting parks instead of individual windmills.

3.1. Satellite Imagery Conversion

In order to be sure we could re-use our code we decided to re-project the satellite file to the World Geodetic System 1984 - WGS84 (EPSG:4326)

```
gdalwarp -t_srs EPSG:4326 in_f out_f
```

This also proved necessary due to the warped nature of the raw satellite imagery. By re-projecting the imagery to a fixed coordinate space, we could easily switch between coordinates and pixel positions by using existing libraries.

3.2. Dataset Creation

As mentioned before, the dataset from which we started is Sentinel satellite imagery. Since we did not have any labeled data, we had to create one ourselves.

3.2.1. MANUAL LABELING

To create a manual labeled set, we gathered a collection of coordinates including boats, land, and windmills. This can be easily done in mapping software (e.g., QGIS). Once we had our set of coordinates, we could start training the model. The model would extract tiles at the mentioned coordinates and use those images as training data. We quickly noticed that the amount of samples was not enough (around 150). So we looked at a way of increasing the number of samples.

3.2.2. ASSISTED LABELING

The issue with our first data set was that its size caused a lot of wrong identifications. This bad model actually gave us a great way of creating more samples. We expanded the number of samples we had by saving all the right and wrongly identified windmills. To include data like oceans and beaches, we would randomly sample at different locations. To ensure a high quality of our samples, we also review each one to make sure they clearly identified the object they were representing and that they were centered.

To reduce loading times, we would save each sample as an image instead of a coordinate, making it possible to load our data set without the need for the original satellite image.

One might notice a large difference between the number of samples (fig. 1) per category. This was largely due to us wanting to initially train a model that could differentiate between land and non-land images. Due to difficulties in training said model, samples of land would not be used in

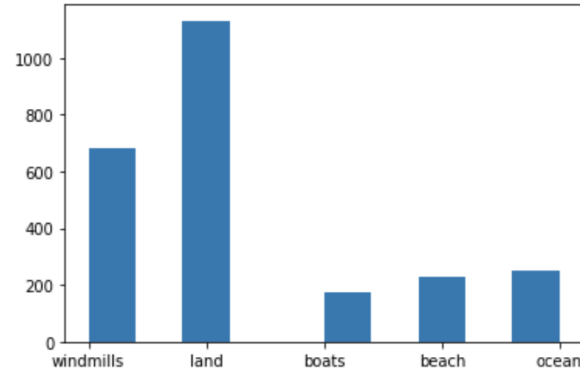


Figure 1. Statistics of final data set showing the number of examples of each category of classification class

the final result. We instead tried to have an even amount of samples representing windmill and non-windmill tiles.

3.3. Noise reduction using OpenCV

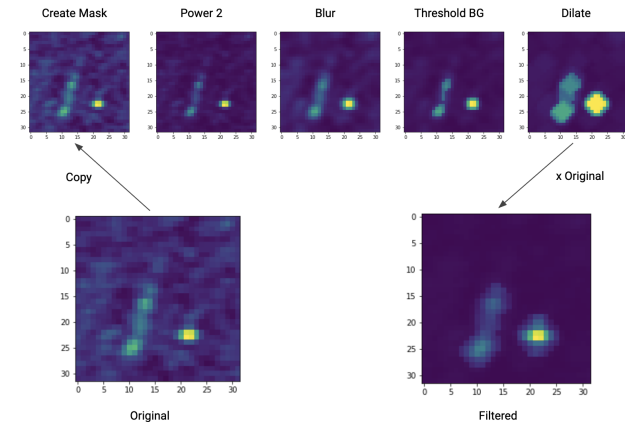


Figure 2. Step by step process of removing noise from a tile containing a single windmill example

We noticed that depending on where the image was acquired, the intensity of the image might be significantly different. To address this, we would pre-process all images before feeding them to our neural network. By masking images in our data set, we noticed a more consistent result in training. Without the mask, it was noticeable that when adding new samples our model would randomly train better or worse. By masking we would get more consistent results; however, this was not empirically tested.

The masking itself was done using the OpenCV library. It

110 consists of 4 steps (fig. 2):

- 111
- 112 • Take the power, increasing highlights and decreasing
113 the background.
 - 114 • Apply blur with a 3×3 kernel, removing small artifacts
 - 115 • Remove the background by nullifying values below the
116 avg value
 - 117 • Dilate remaining shapes with a 3×3 kernel, twice, to
118 ensure edges are included

119 We would then multiply the mask with our original image
120 creating a nice mask around the windmill or boat tile. When
121 using land or ocean imagery, we noticed that this would
122 amplify the amount of noise (fig. 11).

123 3.4. Labeling ocean objects using a CNN

124 3.4.1. OPTIMAL NETWORK

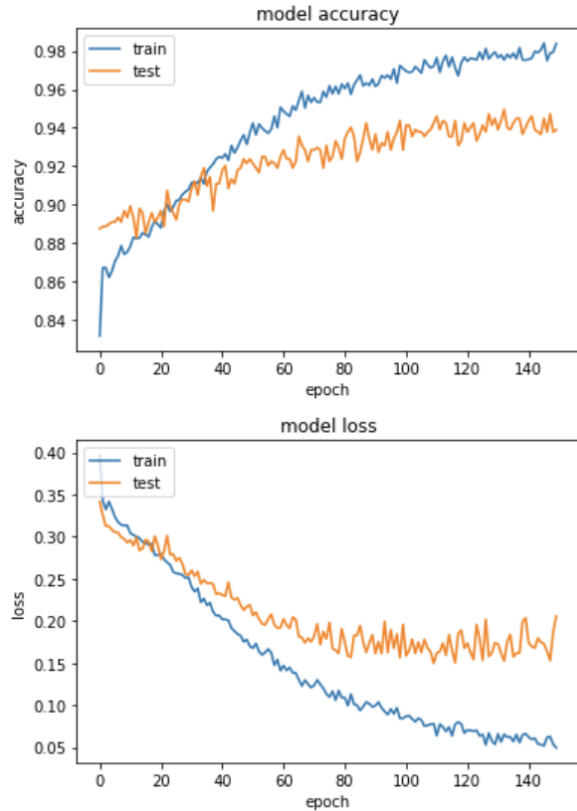
125 Before we started designing the topology of our neural
126 network, we first looked online to see if there were any
127 example typologies that would be usable for our application.
128 One article we found showed a working neural net to
129 identify boats (Moraite, 2019). While the article used
130 optical satellite imagery and we are using a single channel,
131 the network itself was a good basis to build on. The network
132 however, did not produce that good of a result. We suspect
133 that this is due to the very different shapes that windmills
134 and ships can have depending on where and when the image
135 was taken.

136 By tweaking the hyper-parameters, however, and increasing
137 the number of filters to store more information in our
138 network, we were able to train a satisfactory model. We
139 tweaked our parameters in a way that our model would be
140 able to detect most windmills and boats but exclude any
141 beaches or other artifacts present in the ocean. Each
142 convolutional layer uses relu as its activation function. Our
143 model had less artifacts when using a 2-class output; this is why
144 we reduced our network to two final nodes, using sigmoid
145 in the final step. The topology is as follows:

- 146 • $\text{Conv2D}(\text{filters} = 32, 5 \times 5)$
- 147 • $\text{Pool2D}(2 \times 2)$
- 148 • $\text{Conv2D}(\text{filters} = 64, 5 \times 5)$
- 149 • $\text{Pool2D}(2 \times 2)$
- 150 • $\text{Flatten}()$
- 151 • $\text{Dropout}(\text{factor} = 0.5)$

- 152 • $\text{Dense}(n = 2)$

153 All steps contribute to the stable training of our model. The
154 introduction most notably fixed our issue of over-fitting that
155 was initially noticeable with our small data set. For our
156 results we settled on using the weights at 75 epochs, the
157 moment that our loss would stop decreasing (fig. 3) for our
158 test set.



159 *Figure 3. Training statistics of our final model*

160 Looking at our confusion matrix (fig. 4) we see that the
161 model occasionally makes mistakes, but these will be filtered
162 away in the next step of our pipeline. One might notice that the amount of water-class examples is less than
163 the object-class. This difference is due to the fact that examples of ocean tiles are mostly noise. Adding more noisy
164 ocean tiles did not improve our results, so we did not extract any more samples. SAR imagery is inherently noisy; it's called speckle in SAR.

165 3.4.2. ALTERNATIVE: MULTI-CLASS

166 As we mentioned we chose to train our model on two classes
167 instead of the original 5 we designed our dataset for. For
168 completeness sake we included the results of our initial

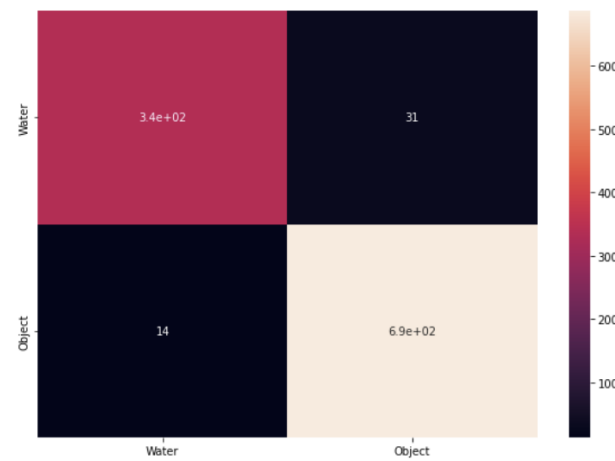


Figure 4. Confusion matrix of our final CNN

network using 5 classes. The training results look similar; however we achieve significantly lower accuracy and much higher loss in comparison to using two classes (fig. 6). Also note that land examples are excluded since land noise looks very similar to ocean noise and would decrease our accuracy even more.

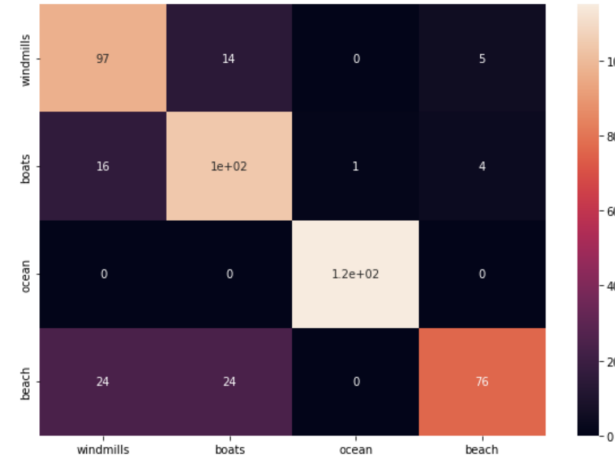


Figure 5. Confusion matrix using the same topology as our best performing network but modified for multi-classification

Looking at the confusion matrix we can see that it is hard to differentiate beaches from boats and windmills. This is an issue that is hard to resolve since beaches have random patterns that sometimes produce artifacts approximating what one would identify as a boat or windmill.

What one can also notice is that boats and windmills can be

differentiated quite well. However, we noticed in later tests that the shape of windmills varies greatly between satellite snapshots and that in reality windmills will have a boat-like shape in most cases.

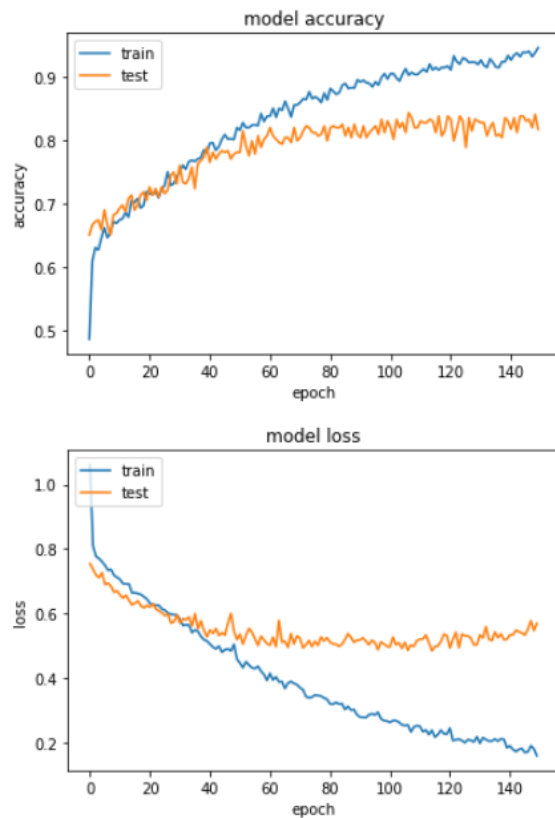


Figure 6. Training results when using multiple classes

3.4.3. ALTERNATIVE: DIFFERENT TOPOLOGY

We experimented with a lot of different typologies. But in all cases we got worse results while training. One of the ideas was that our network should perform better when we gradually densify all our nodes to the final two nodes. The network itself is identical to the final model; however, we replace the last step where we dense in to two nodes with multiple dense layers (128, 64, 16 and 2). This gave us a better result on our training set but did not improve accuracy (fig. 7).

Another attempt was to build a network using a small amount of filters compared to our original network, 6 and 16 compared to 32 and 64. The model quickly perfected the identification of training samples but performed awfully on our test set (fig. 8).

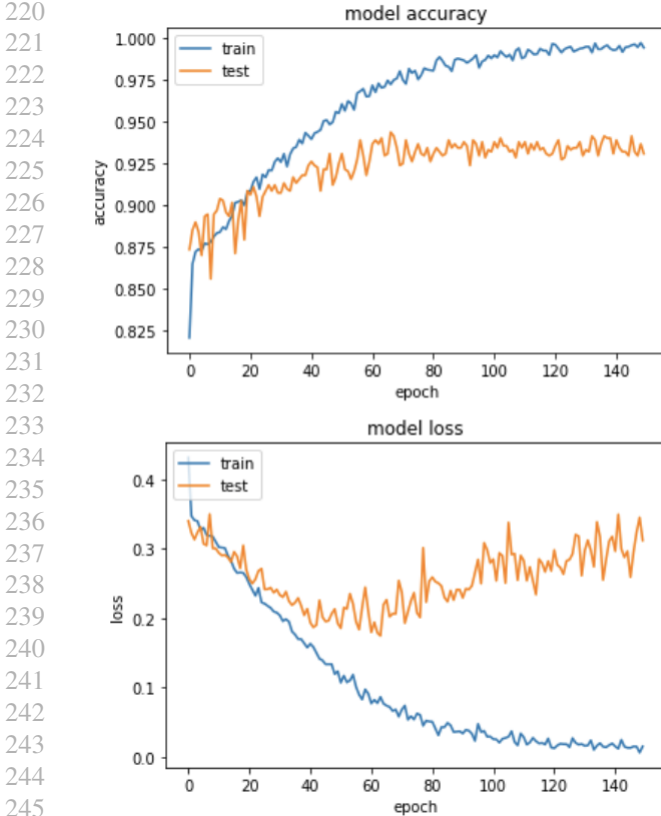


Figure 7. Alternative approach to CNN using multiple dense layers

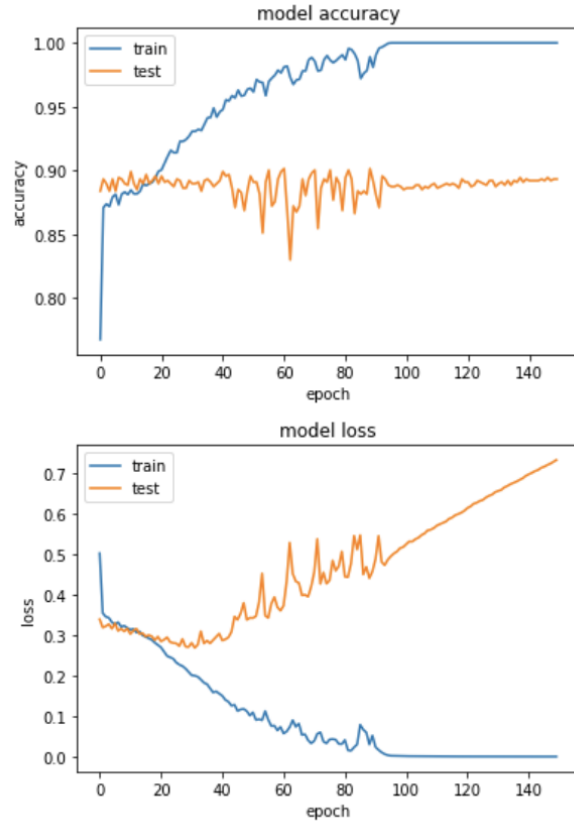


Figure 8. Alternative approach to CNN using less filters

3.5. Detecting Ocean Tile

Since land has buildings which show up as rectangular objects in our satellite imagery, this was labeled in most cases as being a ship/windmill. We had to remove land images from our data set to be able to train our model correctly.

Our first approach was to train a different neural network that would differentiate between land and ocean. This however, seemed like a bigger task than we initially thought and we gave up on the idea after not achieving any good results. We tried to follow a method described by the University of Chinese Academy of Sciences ((Hu et al., 2018)) but quickly realized this was beyond the scope of this project.

We started looking at different tools we could use to accurately define areas that are oceans. We found a project provided by Copernicus that has generated a land coverage map of every area on earth ((cop)). By downloading a segment a using the imagery as a bitmap for masking oceans, we can quickly exclude any tile that can't be a wind-

mill. We added some padding to the edges of land bodies to make sure beach features get excluded, but this is not a reliable way of excluding beaches as beaches can vary on time-related factors like tides.

3.6. Clustering of ocean instances

3.6.1. COMPARING CLUSTERING ALGORITHMS

As we expect to see multiple windmills per park, we can exclude the outliers. Boats or even anomalies detected in the ocean can be removed by using the proper clustering technique. Ordering points to identify the clustering structure (OPTICS) and density-based spatial clustering of applications with noise (DBSCAN) are algorithms for finding density-based clusters in spatial data. We assume the number of clusters relatively low and the density of the clusters rather similar; therefore we tend to use the DBSCAN technique. However we tried the OPTICS clustering method as well with multiple values for the hyper-parameters.

It is clear that the DBSCAN clustering technique produced a result much more in the line we'd expect.

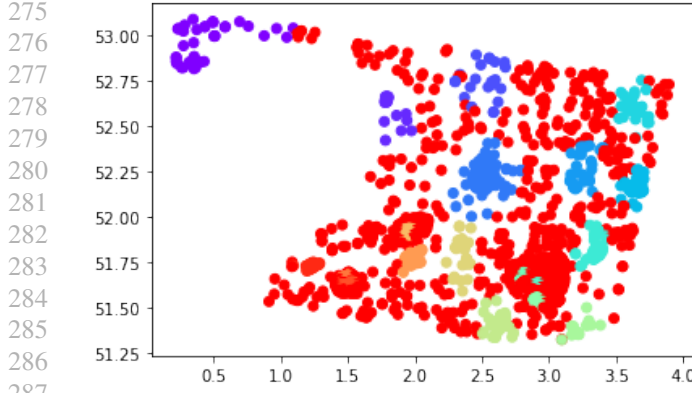


Figure 9. OPTICS clustering result

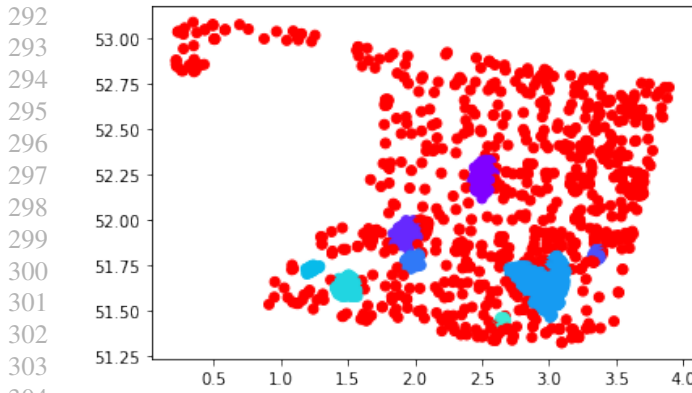


Figure 10. DBSCAN clustering result

4. Results

4.1. Filtering clustered objects

Since clustering is an expensive operation and greatly depends on the distribution of points, we first filter our set of result points to remove densely packed zones. We do this by saving all coordinates containing a windmill/boat in a map and checking for each point we add if it has any neighbors, if so it will skip adding this point. By using a map, this algorithm has a logarithmic complexity making it feasible to parse large zones like the North Sea. An comparison of how windows don't overlap can be seen in Figure 12.

4.2. Final results

We parsed satellite images east of England, west of Denmark and south of China. Looking at the final results (fig. 13) we saw all windmill parks being marked as one. Clusters of boats were also labeled as parks, but these could be filtered when parsing the same area twice at different timestamps

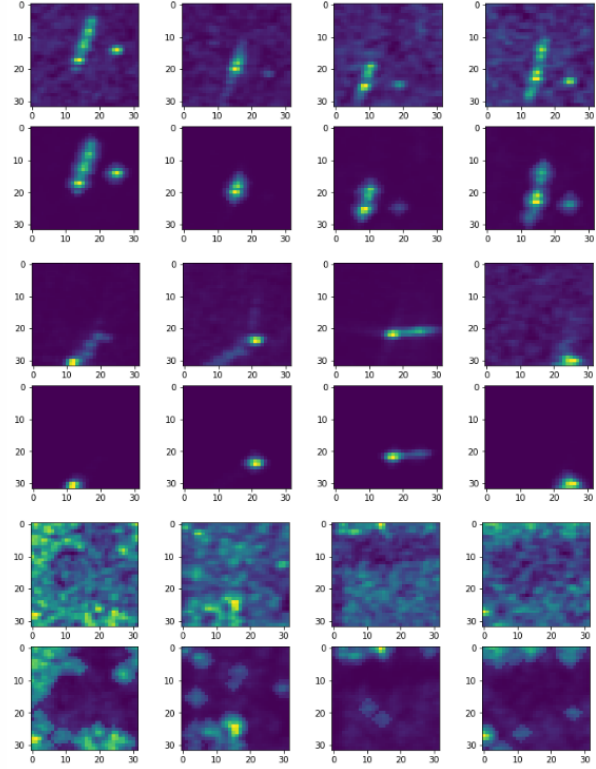


Figure 11. A comparison between noise reduction showing windmills, boats and land based imagery.

and retaining only parks that existed in both snapshots.

4.3. Exceptions

Our model did not perform equally on every case we tested (fig. 14). Coastal areas around Denmark that are periodically flooded are considered "ocean" even though beaches are clearly visible. These areas were still included in our parser which caused beaches to be labeled as windmill parks. One option for resolving this would be to expand borders or try to detect beaches separately from windmills/boats.

The second case in which our detection fails is when a large amount of boats are present. This is notable in parsing the Chinese coast (fig. 14). When a large amount of boats are clustered in an area, the clustering will label this as a park. This could be avoided by filtering based on time, but since harbors are always densely packed a more thorough way of filtering might be needed.

330
331
332
333
334
335
336
337
338
339
340
341
342
343
344
345
346
347
348
349
350
351
352
353
354
355
356
357
358
359
360

Figure 12. Squares indicate a detected windmill, in the left picture every windmill is plotted, on the right we first ran our filtering algorithm to include any close neighbors before adding them to our results.

5. Conclusion

All in all, we are satisfied with this result. The combination of a neural network and a clustering technique resulted in a relatively good detection method. We can detect wind parks in the North Sea area, with only very few false positive polygons - which are dense clusters of boats. The model and clustering techniques performed extremely well in the Skagerrak area, in stark contrast with the results in Chinese waters, where our model performs very poorly. Possibly due to the different orientation of the windmills, but further research is needed to know more about this issue.

5.1. Future Work

In order to distinguish boats from windmills we might think of using the same pictures with another timestamp. Moving objects are most likely boats and we expect to have a much better final result; however the computation load will increase. Using Sentinel's API in order to download new images automatically in order to set up a fully automated system might be something to consider for achieving a state-of-the-art way of identifying windmill parks.

361
362
363
364
365
366
367
368
369
370
371
372
373
374
375
376
377
378
379
380
381
382
383
384

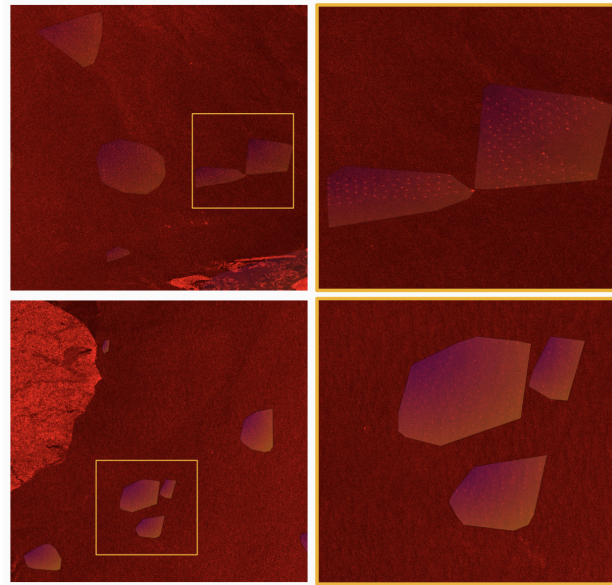


Figure 13. Final result of our algorithm parsing west of Denmark (top) and east of England (bottom). Right images shows an enlarged view clearly showing how the clustering creates a boundary even when parks are close to each other.

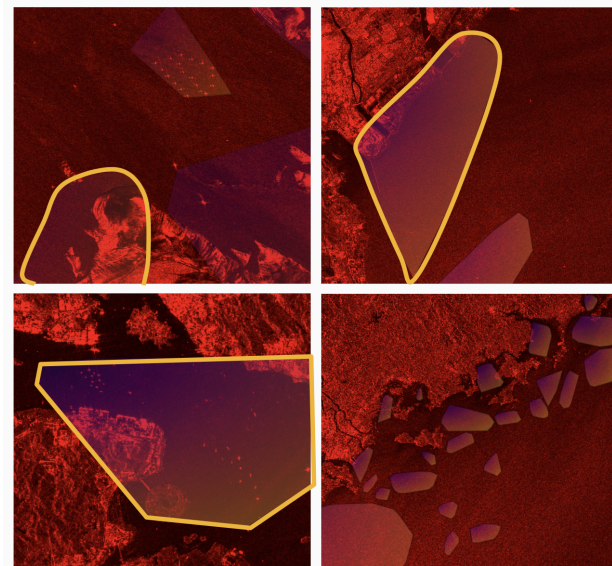


Figure 14. Model performing not as expected in coastal areas in Denmark (top) and harbors around China (bottom).

References

- 385
386 Copernicus land monitoring service. <https://land.copernicus.eu>. Accessed: 2021-12-23.
387
388
389 Deep learning for rare energy infrastructures in satel-
390 lite imagery. [https://bigdata.duke.edu/projects/deep-learning-rare-energy-](https://bigdata.duke.edu/projects/deep-learning-rare-energy-infrastructures-satellite-imagery)
391 [infrastructures-satellite-imagery](https://bigdata.duke.edu/projects/deep-learning-rare-energy-infrastructures-satellite-imagery),
392 2020a.
393
394
395 Github deep learning for rare energy infrastructures
396 in satellite imagery. <https://dataplus-2020.github.io>, 2020b.
397
398 Hu, Y., Zhang, Q., Zhang, Y., and Yan, H. A deep con-
399 volution neural network method for land cover map-
400 ping: A case study of qinhuangdao, china. *Remote*
401 *Sensing*, 10(12), 2018. ISSN 2072-4292. doi: 10.3390/
402 [rs10122053](https://www.mdpi.com/2072-4292/10/12/2053). URL <https://www.mdpi.com/2072-4292/10/12/2053>.
403
404
405 Moraite, D. Detecting ships in satellite imagery, Apr
406 2019. URL <https://medium.com/dataseries/detecting-ships-in-satellite-imagery-7f0ca04e7964>.
407
408
409 Sagar, A. Deep learning for ship detection and segmen-
410 tation. <https://towardsdatascience.com/deep-learning-for-ship-detection-and-segmentation-71d223aca649>, Nov 2019.
411
412
413
414
415
416
417
418
419
420
421
422
423
424
425
426
427
428
429
430
431
432
433
434
435
436
437
438
439